THE INFLUENCE OF MATERIAL PROPERTIES ON THE WIRE SAWING PROCESS OF MULTICRYSTALLINE SILICON

Thomas Kaden*, Elena Ershova, Lydia Lottspeich, Marcel Fuchs
Fraunhofer Technology Center for Semiconductor Materials, Am St.-Niclas-Schacht 13, 09599 Freiberg, Germany
*Corresponding author: thomas.kaden@thm.fraunhofer.de

ABSTRACT: The influence of material properties on the cutting efficiency of multicrystalline silicon was investigated for bricks taken from different positions of industrial-scale G5 multicrystalline silicon ingots in a diamond wire sawing process. It is shown, that bricks from diverse ingot positions reveal significant differences regarding the forces in feed direction when exactly the same process conditions are applied. Higher forces in feed direction imply a stronger bowing of the wire web developing during the process and therefore indicate a lower cutting efficiency. The size of silicon nitride and silicon carbide precipitates in the material are identified as the main factor for the cutting efficiency. The findings show the potential to optimize industrial wafering processes regarding process time or wire consumption.
Keywords: Wafering, diamond wire, multicrystalline silicon, characterization

1 INTRODUCTION

For the production of solar cells from multicrystalline silicon (mc-Si) the so-called High Performance (HP) mc-Si is the state-of-the-art base material. Using n-type HP mc-Si, record conversion efficiencies were recently demonstrated [1]. Even though this material shows a superior electrical quality compared to standard mc-Si, there are still crystal defects and impurities present, which might influence the cutting efficiency in multi wire sawing. Especially for the technology transition in the field of wire sawing of crystalline silicon from slurry to diamond wire sawing (DWS), the material properties of mc-Si are a critical factor. At the time, DWS processes of mc-Si require about 40% more process time compared to Cz-Si.

While many phenomena in the DWS abrasion process are already understood [2-4], the material properties of mc-Si with respect to the cutting efficiency were not investigated in detail yet. In this contribution major material influences in bricks of HP mc-Si were investigated and compared with Czochralski silicon.

2 PRE-CHARACTERIZATION OF BRICKS

2.1 Brick position

The investigations were performed on bricks with a height of 295 mm and a base area of 156 mm x 156 mm taken from different positions of a G5 HP mc-Si ingot. The bricks are named according to Fig. 1. A corner brick is defined by two faces having contact with the crystallization crucible, an edge brick has one such face and a center brick has no contact with the crucible. There are nine such center bricks in a G5 mc-Si ingot. A monocrystalline Czochralski ingot (Cz-Si) was used as reference. All bricks were boron doped.

2.2 Identification and electrical characterization

Since the investigated bricks originate from the same ingot, the doping concentration should be equal in all bricks. This was confirmed by four-point probe measurements of the resistivity. As shown in Fig. 2, the resistivity is in the range of 4 – 10 Ω cm corresponding to a boron doping concentration of $(1.4 – 3.5)\cdot10^{15}$ cm^{-3}. The resistivity of the reference Cz-Si brick is 1.3 – 1.7 Ω cm ($8.6\cdot10^{15} – 1.1\cdot10^{16}$ cm^{-3}).

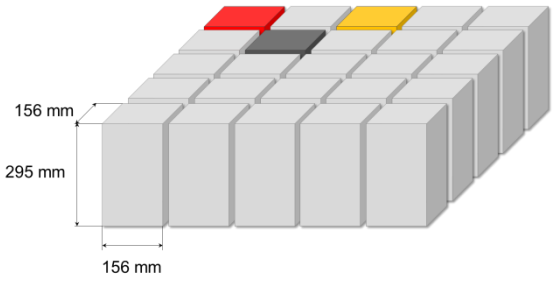

Figure 1: Scheme of brick positions in G5 mc-Si ingots (center – grey, edge – orange, corner – red).

The position of the bricks in the ingot was unambiguously determined by minority carrier lifetime measurements on bottom and top slabs of the bricks. The topographic measurements clearly show areas of reduced lifetime near the crucible (the so-called "red zone") which indicates the position in the ingot.

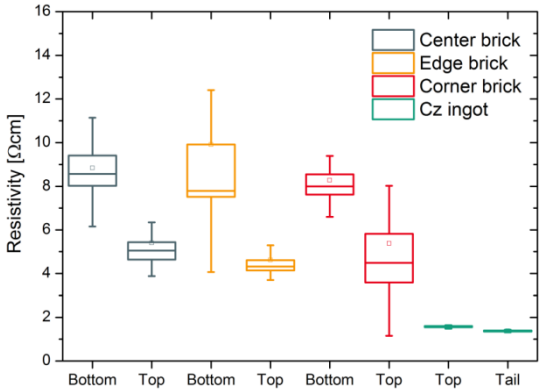

Figure 2: Resistivity of the investigated bricks, measured at the bottom and top, respectively.

2.3 Brick inspection by IR transmission

The HP mc-Si bricks were inspected prior to diamond wire sawing by IR transmission. The used method offers a lateral solution of 200 µm, i.e. inclusion with dimension larger than 200 µm can be found. As it can be seen from Fig. 3, there are no inclusions present in the three bricks, which allows for the application of an industrial wafering process.

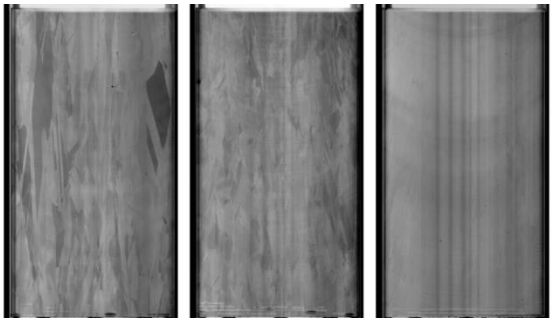

Figure 3: IR transmission inspection of the mc-Si bricks, corner (left), edge (middle) and center (right) position.

3 DIAMOND WIRE SAWING

3.1 Process parameters

The DWS processes were conducted on a Meyer Burger DS264 industrial wire saw in oscillating mode. In order to compare the cutting efficiency for the bricks from different ingot positions, the same process parameters were applied for cutting bricks of 295 mm, respectively. The parameters are summarized in Tab. 1.

Table 1: Process parameters of the diamond wire sawing experiments.

Process parameter	Value
Wire core diameter	120 µm
Diamond grit size	8-16 µm
Pitch	330 µm
Feed rate	0.55 mm/min
Wire speed	18 m/s
Wire tension	28 N
Wire consumption	3 m/wafer
Cooling medium	water
Additive concentration	2%

3.2 Cutting efficiency

During the sawing process, the forces in three directions (parallel and perpendicular to the wire direction, in feed direction) are permanently recorded. Since equal process parameters were used for all investigated bricks, the forces measured during the wire sawing process can be used to evaluate the cutting efficiency. Especially the force in feed direction F_z is an appropriate measure for the evaluation. When the cutting efficiency is low, a higher bowing of the wire web beneath the brick occurs, which results in a higher F_z.

In Fig. 4, the F_z values recorded over the whole process time are displayed for all bricks. It is found that the center brick reveals the highest F_z during cutting, while F_z for the edge and corner bricks is significantly lower. The highest cutting efficiency (lowest F_z) is found for the Cz-Si reference, as it would be expected. However, F_z for the edge and corner bricks is only 11-18 % higher compared to the Cz-Si reference. Thus, DWS processes using almost the same feed rate as for Cz-Si would be possible for these bricks. It should be emphasized that two-thirds of a G5-ingot are edge and corner bricks.

3.3 Wafer geometry and quality

The DWS processes are further evaluated by the quality of the produced wafers. In Tab. 2, the average wafer thickness and the total thickness variation (TTV) of the wafers are shown.

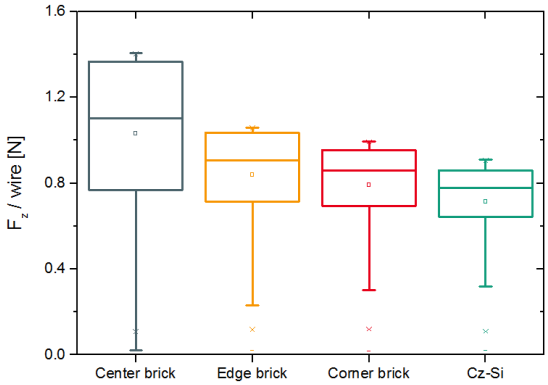

Figure 4: Force in feed direction (F_z) recorded during the entire DWS processes for the different bricks.

The lowest wafer thickness was measured for the reference Cz-Si, while the wafers from the mc-Si center brick yield the highest thickness. The thickness of wafers from the edge and corner bricks is in between the values of center brick and Cz-Si. This is in good agreement with the measured F_z values. The higher F_z is throughout the process, the higher is the wire wear, i.e. the effective wire diameter decreases by an enhanced loss of diamond volume. This leads to a reduction of the sawing channel width resulting in thicker wafers.

The TTV shows a similar trend, the higher the mean value of F_z, the higher is the TTV. It should be mentioned that the TTV for the Cz-Si reference is increased in spite of the given trend. This can be explained by the pseudo-square geometry of the Cz-SI ingot, for which the sawing process was not optimized.

Table 2: Mean values of F_z during the DWS process, wafer thickness and total thickness variation (TTV).

Brick position	Mean F_z/wire [N]	Mean wafer thickness [µm]	TTV [µm]
Center	1.03	192.2	17.7
Edge	0.84	190.1	15.2
Corner	0.79	188.9	14.8
Cz-Si (ref.)	0.71	188.6	16.8

3.4 Mechanical stability of the wafers

It was tested if the differences in the cutting efficiency are also reflected in the mechanical stability of the wafers. The four-line bending test was used to test as-sawn and damage etched wafers. There was no difference detectable for both wafer states.

4 MATERIAL PROPERTIES AND RELATION TO THE CUTTING EFFICIENCY

In order to identify the major material parameter that dominates the cutting efficiency, different material properties were investigated and are discussed in the following.

4.1 Carbon and oxygen concentration

The concentration of dissolved substitutional carbon (C_s) and interstitial oxygen (O_i) was determined by Fourier Transform Infrared Spectroscopy (FTIR) in the bottom and top slabs of the mc-Si bricks and in the top and tail slaps of the Cz-Si brick, respectively. As depicted in Fig. 5, there are no significant differences in the O_i-concentration of the mc-Si bricks. The same holds for the Cs-concentration, see Fig. 6.

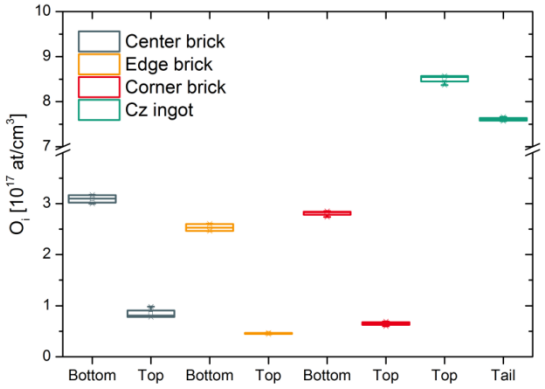

Figure 5: Concentration of interstitial oxygen (O_i) in the different HP mc-Si bricks and the Cz-Si reference.

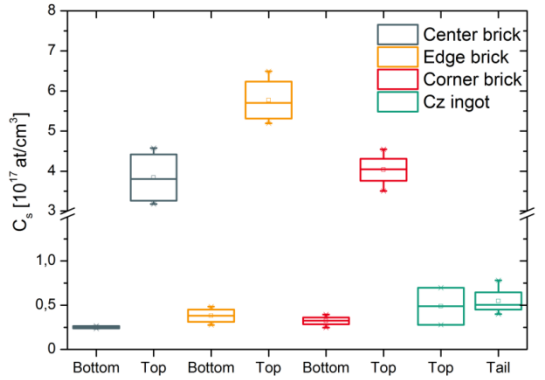

Figure 6: Concentration of substitutional carbon (C_s) in the different HP mc-Si bricks and the Cz-Si reference.

Thus it can be concluded that the cutting efficiency of mc-Si does not depend on the O_i- or C_s-concentration in the concentrations commonly present in the material.

4.2 Grain structure

The grain structure was characterized using X-ray Diffraction (XRD) with respect to the number of grains on a wafer, the occurring crystal orientations and the type of grain boundaries. Thy typical characteristic of HP mc-Si is found, in the bottom of the bricks there is a high number of grains with a small area. The grains are growing in area towards the top of the ingot, the number of grains decreases consequently.

The smallest grains are found in the center brick, where the most pronounced growth in grain size is observed. Since the mean value of the grain size is almost equal for each brick, no influence of the crystal structure on the sawing performance is expected within a single ingot.

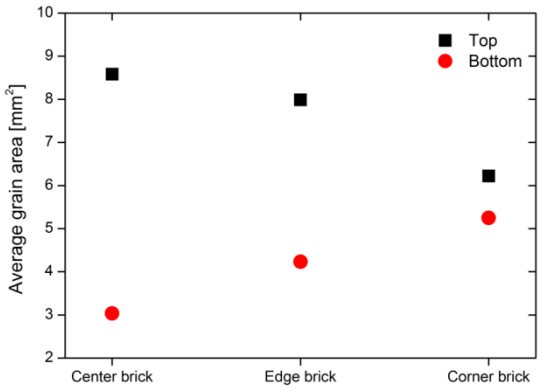

Figure 7: Mean grain area measured on the bottom and top slab of each ingot.

4.3 Precipitates

Precipitates were detected by IR transmission microscopy on the bottom and top slabs of the bricks. In Fig. 8, examples of silicon nitride precipitates (Si_3N_4) occurring as needles are shown. These precipitates are randomly oriented in the silicon crystal as Fig. 8 illustrates. Thus one can display them along the needle or as cross section of the needle. Furthermore, silicon carbide precipitates were found in less extent.

In order to evaluate the influence of the precipitate size on the cutting efficiency, the number of precipitates was automatically counted on slabs of each brick in an area of 10 x 10 cm²; the area of each precipitate was measured. A significant difference of the mean precipitate area between the center and the corner and edge bricks was found.

The values of the mean force F_z in the sawing process and the related mean area of precipitates are summarized in Tab. 3. Although there is a clear difference between the center brick and the bricks near the crucible wall, the correlation is still poor and needs to be improved with a higher number of experiments. The convolution of the precipitate density and the area could also lead to a better correlation and will be conducted in future investigations.

However, it is reasonable to consider the existent Si_3N_4- and SiC-precipitates as the main factor reducing the cutting efficiency in mc-Si since both materials have a higher hardness and fracture toughness compared to silicon, respectively.

It should be mentioned that the situation might be different in the case of other crystal producers. If the precipitates in the edge regions of the ingot would be larger, depending on the melt convection during the crystallization process, the cutting efficiency of edge and corner bricks will be lower compared to center bricks.

Table 3: Mean values of F_z during the DWS process, wafer thickness and total thickness variation (TTV).

Brick position	Mean F_z/wire [N]	Mean area of precipitates [µm²]
Center	1.03	95.7
Edge	0.84	53.2
Corner	0.79	44.3

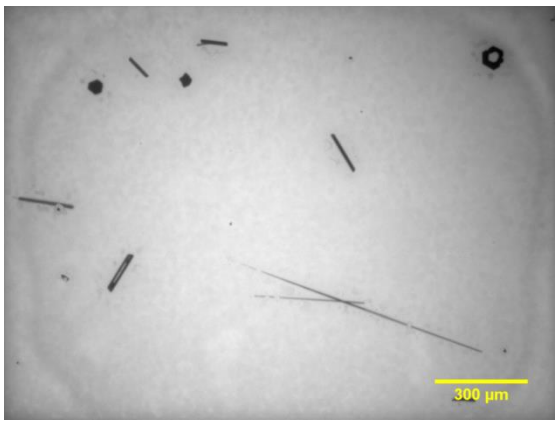

Figure 8: IR transmission microscopy of the edge brick showing silicon nitride needles in longitudinal sense and as cross section.

5 CONCLUSION

The inspection and characterization of multicrystalline silicon is important for the optimization of the diamond wire sawing (DWS) process. It turned out that the standard IR transmission inspection with 200 µm spatial resolution is not sufficient to detect all impurities, which have a relevant influence on the cutting efficiency of the DWS process.

By comparing bricks from different ingot positions, significant differences in the cutting efficiency were found, as demonstrated by the force in feed direction recorded over the entire process time. For a specific crystal manufacturer within this work, the bricks from the edges and corners of an HPM-Si ingot can be easier cut compared to bricks from the ingot center. This was mainly attributed to the presence of silicon nitride precipitates of different size within these ingots as characterized by IR transmission microscopy.

The findings presented here offer the potential for process optimization with a cost reduction potential. Consequently, a presorting of bricks prior to the wafering could be established, which distinguishes center and edge/corner bricks, given that the precipitate distribution is known. After presorting, adapted processes regarding feed rate or wire consumption can be applied for the two groups of bricks.

The relevant precipitate distribution can be monitored with a high resolution IR transmission measurement of the bricks, offering a spatial resolution of 18 µm.

In general, a further reduction of the size of precipitates, especially of silicon nitride needles and SiC clusters is desired to further improve the cutting efficiency of multicrystalline silicon bricks in diamond wire sawing and thereby narrow the gap with respect to DWS processes on solar Cz-Si.

REFERENCES

[1] J. Beneck et al., “High-efficiency n-Type HP mc Silicon Solar Cells”, IEEE Journal of Photovoltaics, Vol. 7, No. 5, pp. 1171-1175 (2017).

[2] H.J. Möller, “Basic Mechanism and Models of Multi-Wire Sawing”, Advanced Engineering Materials, Vol. 6, No. 7, pp. 501-513 (2004).

[3] R. Buchwald et al., “Analysis of the sub-surface damage of mc- and Cz-Si wafers sawn with diamond-plated wire”, Energy Procedia, Vol. 38, pp. 901-909 (2013).

[4] S. Würzner et al., “Characterization of the Diamond Wire Sawing Process for Monocrystalline Silicon by Raman Spectroscopy and SIREX Polarimetry”, Energies, Vol. 10, 414 (2017).

ACKNOWLEDGEMENT

Part of this work was funded by the German Ministry for Economic Affairs and Energy (BMWi) within the project “DIANA” (Contract No. 0324087B), which is gratefully acknowledged.